A simple miniature optical spectrometer with a planar waveguide grating coupler in combination with a plano-convex lens

Kalyani Chaganti, Ildar Salakhutdinov, Ivan Avrutsky, Gregory W. Auner

Department of Electrical and Computer Engineering, Wayne State University, Detroit, MI-48202.
kalyani@wayne.edu

Abstract: A miniature optical spectrometer with a thin-film planar waveguide grating coupler in combination with a miniature plano-convex focusing lens has been investigated. With optical part of the spectrometer as small as 0.2 cubic cm, the spectral resolution varies from 0.3 nm to 4.6 nm within the wavelength range 488.0 nm – 632.8 nm.

OCIS codes: (230.0230) Optical devices; (230.3120) Integrated optics devices; (350.3950) Micro-optics.

References and links

1. M.Varasi, M. Signorazzi, A. Vannucci and J. Dunphy, "A high-resolution integrated optical spectrometer with applications to fibre sensor signal processing," Meas. Sci. Technol. **7** , 173-178 (1996).
2. H.L. Kung, S.R. Bhalotra, J.D. Mansell, D.A.B. Miller and J.S. Harris Jr., " Standing-wave transform spectrometer based on integrated MEMS mirror and thin-film photodetector," IEEE J. Sel. Top. Quantum. Electron. **8,** 98-105 (2002).
3. H. Stiebig, D.Knipp, S.R. Bhalotra, H.L. Kung and David A.B. Miller, "Interferometric sensors for spectral imaging," Sens. Act. A **120**, 110-114 (2005).
4. Dietmar Sander and Jorg Muller, "Selffocusing phase transmission grating for an integrated optical microspectrometer," Sens. Act. A **88**, 1-9 (2001).
5. G. Lammel, S. Schweizer and Ph. Renaud, "Microspectrometer based on a tunable optical filter of porous silicon," Sens. Act. A **92**, 52-59 (2001).
6. J.H. Correia, G. de Graf, M. Bartek and R.F. Wolffenbuttel, "A single-chip CMOS optical microspectrometer with light-to-frequency converter and bus interface," IEEE J. Solid-State Circuits **37,** 1344 – 1347 (2002).
7. R.F. Wolffenbuttel, "State-of-the-art in integrated optical microspectrometers," IEEE. Trans. Instrum. Meas. **53**, 197-202 (2004).
8. Don.S.Goldman, P.L.White, and N.C. Anheier, "Miniaturized spectrometer employing planar waveguides and grating couplers for chemical analysis," Appl. Opt. **29**, 4583-4589 (1990).
9. S. Ura, F. Okayama, K. Shiroshita, K. Nishio, T. Sasaki, H. Nishihara, T. Yotsuya, M. Okano and K. Satoh, "Planar reflection grating lens for compact spectroscopic imaging system," Appl. Opt. **42**, 175-180 (2003).
10. D.Brennan, J.Alderman, I.Sattler, J.Walshe, J. Huang, B.O Connor and C. O. Mathuna, "Development of a microspectrometer system for process control application," Infrared Phys. Technol. **43**, 69-76 (2002).
11. O. Manzardo, H.P.Herzig, C.R.Marxer and N.F. de Rooij, "Miniaturized time-scanning Fourier transform spectrometer based on silicon technology," Opt. Lett. **24**, 1705-1707 (1999).
12. S.H. Kong, D.D.L. Wijngaards, R.F. Wolffenbuttel, "Infrared micro-spectrometer based on a diffraction grating," Sens. Act. A **92,** 88-95 (2001).
13. Pavel Cheben, Ian Powell, Siegfried Janz and Dan-Xia Xu, "Wavelength-dispersive device based on Fourier-transform Michelson-type arrayed waveguide grating," Opt. Lett. **30**, 1824-1826 (2005).
14. Ivan Avrutsky, Kalyani Chaganti, Ildar Salakhutdinov and Gregory Auner, "Concept of miniature optical spectrometer using integrated optical and microoptical components," (submitted to Appl.Opt.).
15. D. Maystre, M. Neviere and R. Petit, "Experimental verifications and applications of the theory," in *Electromagnetic Theory of Gratings*, R.Petit, ed. (Springer, New York, 1980), Chap. 6.
16. D. W. C. So and S. R. Seshadri, "Metal-island-film polarizer," J. Opt. Soc. Am. B **14**, 2831-2841 (1997).
17. M. A. Sletten and S. R. Seshadri, "Thick metal surface-polariton polarizer for a planar optical waveguide," J. Opt. Soc. Am. A **7**, 1174-1184 (1990).

#68838 - $15.00 USD Received 13 March 2006; revised 20 April 2006; accepted 25 April 2006

1. Introduction

Compact, light-weight, rigid miniature spectrometers with no moving parts are needed for a wide variety of applications including bio-sensors and space applications where every inch of payload counts. Miniaturization increases portability and paves way for making in-situ measurements. Applications and miniaturization go hand-in-hand. Applications necessitate miniaturization and miniaturization in turn creates more applications. Miniaturization also eases the integration of micro and miniature spectrometers into other technologies like microelectronics. Miniaturization helps to realize lab-on-a-chip devices and very large scale integrated devices which are the order of the day.

Micro and miniature spectrometers have been developed for the visible [1-9] and infrared ranges [5, 10-13] and have been built using different technologies such as MEMS [2, 5], CMOS [6], MOEMS [11] and integrated optics technologies [4, 8]. Spectrometers in general can be classified based on their underlying principle like grating-based [4, 7-10, 12, 13], Fabry-Perot filter based [5, 6], AOTF-based [1] and Fourier-transform based spectrometers [2, 3, 11] etc. With the advent of integrated optics (IO), microspectrometer researchers were able to combine the different optical elements that constitute a conventional spectrometer to form an integrated device. For example, a single diffractive optic element (DOE) performs the three functions of collimating, spectral dispersion and focusing. Grating-based spectrometers have the advantage of quick read-out which is not the case for tunable filter based spectrometers or Fourier-transform based spectrometers.

Grating-based spectrometers with single dimension of optical part about 1 or 2 cm have been demonstrated to give a resolution (Full width at half maximum or FWHM), $\Delta\lambda$ = 5 nm [9] in a spectral range of 100 nm in the visible range and 10 nm [4] in a spectral range of 300 nm in the visible range. Recently, a very high resolution (0.07 nm) arrayed waveguide grating based spectrometer has been reported in a wavelength range of about 20 nm in the C-band [13]. Two other grating-based visible and infrared microspectrometers of sizes of single dimension only a few millimeters have been demonstrated to give a FWHM of ~ 60nm at 600 nm and ~500 nm at 5 μm respectively [7]. Clearly there is a trade-off between the size of the spectrometer and the spectral resolution it provides.

In Ref. [14], we have introduced the concept of a microspectrometer based on a diffractive optical element (DOE) integrated with a planar waveguide. In the preliminary tests, a holographically fabricated uniform-period grating in combination with a 1cm focal length miniature lens was used to emulate the DOE. For the wavelengths of 514.5 nm and 632.8 nm, the spectral resolution was experimentally found to be 0.5 nm. The sub-nm resolution for a device of about 1 cm in size of single dimension appears to be at least an order of magnitude better than the resolution of microspectrometers described in literature so far. This motivates to study the device operation further i.e., at other wavelengths and in a wide spectral range. Here, we also experimentally determine the resolution of the miniature spectrometer in three different configurations each employing a lens of different focal length.

2. Design of the miniature spectrometer

The uniform-period grating, which is the core element of this miniature optical spectrometer, is a surface relief grating fabricated on a thin-film waveguide designed to be a single mode waveguide in the wavelength range of the miniature spectrometer i.e., 480 nm - 640 nm. Single-mode operation is essential because higher order modes lead to undesirable overlap between different optical waveguide modes within the desired spectral range. The thin-film waveguide employed is a hafnium oxide waveguide on BK7 glass substrate with a cladding layer of silica. The uniform-period grating was designed to have a period of 400 nm. The choice of the grating period depends on the desired out-coupling angles for the targeted wavelength range. For our miniature spectrometer, close-to-normal outcoupling angles are required for the different wavelengths so as to minimize off-axis lens aberrations. The

#68838 - $15.00 USD Received 13 March 2006; revised 20 April 2006; accepted 25 April 2006

outcoupling angles for the targeted wavelength range (480 nm - 640 nm) which depend on the effective index of the waveguide at those wavelengths and the period of the grating vary from ~ 8^o - 33^o for a grating period of 400 nm. A plano-convex focusing lens is placed in an appropriate lens holder which is attached to the waveguide surface such that the lens' optical axis coincides with the normal to the center of the grating. A guided wave confined to the plane of the thin-film waveguide is outcoupled into free-space by the uniform period grating and is then focused by the plano-convex focusing lens. The angle of out-coupling by the grating is different for different wavelengths which in combination with focusing results in spectral resolution. The coupling of the guided wave from the waveguide plane to free-space paves way for building a compact device with high resolution. For this reason, a waveguide grating coupler promises to be a good candidate for the realization of miniature spectrometers.

A CCD camera whose position can be controlled by mini rotation and 3-directional translation screws collects the spectra and sends them real-time to a computer. Integration of several frames is also done by the imaging application to improve the SNR at the output when detecting weak signals thereby improving the overall efficiency of the device.

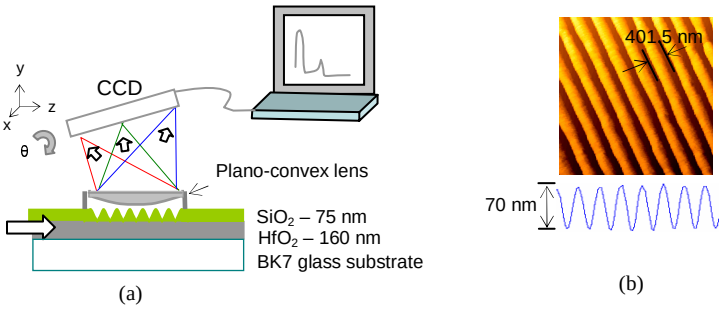

Fig. 1. (a) Integrated-optic and micro-optic combined design of a miniature spectrometer (b) AFM image of the dry etched grating on hafnium oxide waveguide.

3. Fabrication

The detailed fabrication procedure is as follows. Hafnium oxide was chosen for the thin-film waveguides not only because it is hard, chemically and environmentally stable but also because it has a high refractive index (n ~2). Commercially available (Thinfilm Labs) hafnium oxide thin films were deposited by electron beam evaporation to the desired thickness (160 nm) on 1.2 mm thick BK7 glass slides to form thin-film waveguides. A cladding layer of silica of thickness 75 nm was also deposited by e-beam evaporation on these films. Two opposite edges of each of the waveguide samples were prepared by polishing to make the waveguide suitable for edge-coupling.

Waveguide gratings were fabricated by two-beam interference lithography with UV beams at 244 nm. UV5 photoresist diluted (1 part resist, 2 parts dilutant by volume) by EC11 was spin-coated on the waveguide sample (Surface dimensions: 1 inch × 1 inch) at 5100 rpm spin speed for 35 seconds. After soft-baking for 15 minutes in oven at 90^oC, exposure was done with a dose of 30 – 50 mJ/sq.cm. This was followed by post-exposure baking for 1 minute on a hot plate at 110^oC. Then, dunk-developing was done for 35-45 s in LDD 26W developer. After hard-baking for 2 minutes on hot plate at 110^oC, dry etching of the grating pattern on the top silica cladding layer was done in Plasmatherm SLR 770 with flow rates of C_4 F_8 and SF_6 at 8 sccm and 0.5 sccm respectively. The RF1 and the RF2 powers were both 50 Watts and the chamber pressure was 10 mTorr. The duration of the etching process was 20 minutes. The residual resist was removed by acetone and iso-propanol wash. The depth of the etched gratings was between 60-70 nm from atomic force microscope (AFM) image [Fig. 1(b)]. Good surface quality gratings were obtained and the etch depth throughout a grating

#68838 - $15.00 USD Received 13 March 2006; revised 20 April 2006; accepted 25 April 2006

was uniform (confirmed by AFM pictures at several places on the grating). The etch resistivity of UV5 was reasonable resulting in good etch selectivity for silica.

For our experiments, as a starting point, we have targeted a low grating diffraction efficiency of about 7-10%. From [15], we estimated that a grating depth of 70 nm for a holographic grating of period 400 nm would have an efficiency of ~ 7% in the -1 order Littrow mount in TE polarization for λ = 632.8 nm. An efficiency of 7% was achieved in the same configuration with a grating depth of 70 nm for our fabricated gratings agreeing very well with the theoretical estimation. A low diffraction efficiency in this configuration also means a low diffraction efficiency for the transmitted order when light is totally internally reflected in the guiding layer. A very high diffraction efficiency of the transmitted order when light is totally internally reflected in the guiding layer would result in shorter propagation length thereby resulting in lesser off-axis lens aberrations but a shorter propagation length would also result in a greater diffraction-limited spot size which worsens the spectral resolution. A low efficiency on the other hand, gives longer propagation length along the grating and hence there will be more effective number of grooves contributing to dispersion thus resulting in higher resolution. In order to maximize the spectrometer resolution, optimization needs to be done to determine the ideal grating depth and the resolution results from this study would provide a good starting step for the same.

4. Experiments

For our experiments, one very large focal length lens (f = 14 cm) which results in a large size spectrometer (single dimension of optical part < 16 cm) and two other smaller focal length lenses (*f* = 2 cm, 1 cm) which would result in a compact size of spectrometer (single dimension of optical part < 2.5 or 1.5 cm) were chosen. These lenses were assembled one after another at an arbitrary small height (about 5mm, 2mm and 1mm respectively) above the same waveguide grating so that there is no contact with the grating grooves and the resolution was found in all the three set-ups with the help of a pair of wavelengths. Furthermore, with the set-up with the 1 cm lens, resolution was found for several pairs of wavelengths and also for a range of wavelengths with the help of multiple wavelengths within the range. The lenses were mounted such that their optical axes coincided with the normal from approximately the center of the grating. The common uniform-period grating that was employed for all these experiments had a period of 401.5 nm, depth of 70 nm and a footprint of ~ 4 mm × 2.5 mm (with the grooves being oriented along the longer side).

In all the experiments with a pair of wavelengths, laser beams of two different wavelengths were combined at a beam splitter and edge-coupled at the same point into the waveguide by a 10x microscope objective with numerical aperture NA = 0.25. As expected, the guided light beams (TE_0 mode) of different wavelengths were dispersed in different directions by the grating and focused by the focusing lens. Figure 2(a) shows the focused red (632.8 nm) and green (514.5 nm) arcs with the 14 cm lens and Fig. 2(b) shows the same along with the set-up with the 1 cm lens.

#68838 - $15.00 USD Received 13 March 2006; revised 20 April 2006; accepted 25 April 2006

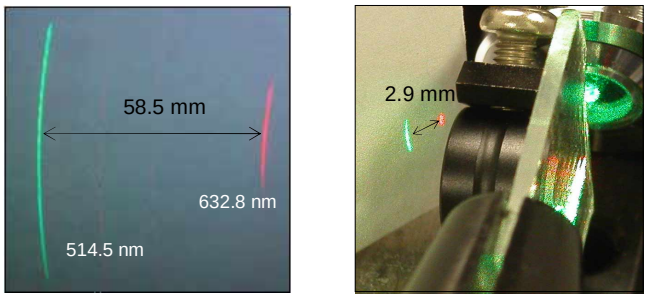

(a) (b)

Fig. 2. (a) Picture of the sharply focused arcs (514.5 nm and 632.8 nm) on a paper screen in the case of ***f*** = 14 cm lens (b) The waveguide and 1 cm lens set-up with the focused red (632.8 nm) and green (514.5 nm) arcs on a paper screen.

A photodetector with slit aperture was moved along the midpoints of the sharply focused arcs to find the resolution in the case of the 14 cm lens. In the cases of the other two lenses, the CCD camera, Prosilica EC 750 (Pixel size: 6μm × 6μm) was used to capture the focused arcs and estimate resolution. Using the real-time image from the computer as a feedback, the position of the CCD was adjusted to give sharp focusing of both the arcs. Even though quantitative information on the CCD position could not be recorded, it was observed that a quick and easy positioning for sharp focusing could be done with the help of the feedback. A Lorentzian fitting of the curves resulting by taking a cross-section along the centers of the arcs was done and linear dependency was assumed between the pixels (or physical distance in the case of the 14 cm lens) and the wavelengths to find the resolution i.e., first the distance between the peaks of the two known wavelengths in pixels was determined exactly and then, simple linear proportionality was applied to convert the FWHM of the wider curve of the two from pixel scale to wavelength scale. This is nothing but $\Delta\lambda$ or the resolution of the miniature spectrometer for this pair of wavelengths.

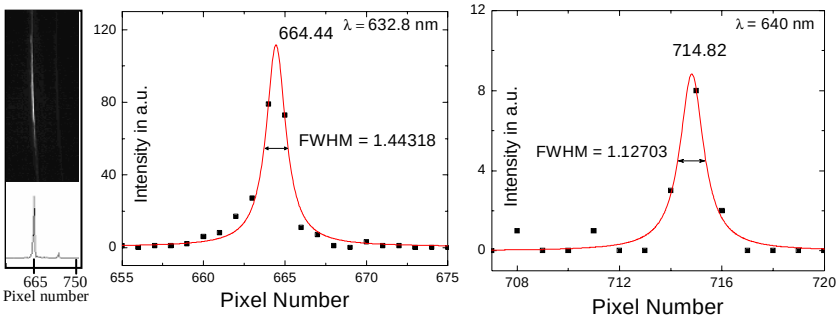

(a) (b) (c)

Fig. 3. With *f* = 2 cm lens (a) A CCD picture of the sharply focused arcs at 632.8 nm (left) and 640.0 nm (right) and the one-dimensional intensity profile along the mid-points of the arcs (b) and (c) Lorentzian approximation of the one-dimensional intensity peaks at 632.8 nm and 640.0 nm respectively.

The background noise was found to be originating very little from the laser light scattering at the grating but predominantly from the CCD camera dark response. Ambient noise was found to be very flat along the pixels and the measured average value was 11 in a.u. This average ambient noise value was subtracted from the actual intensity measurements before doing the Lorentzian fitting and finding the resolution. Figure 3 shows the results for wavelengths of 632.8 nm and 640.0 nm with the set-up with the 2 cm lens. It can be seen in

#68838 - $15.00 USD Received 13 March 2006; revised 20 April 2006; accepted 25 April 2006

these curves [Figs. 3(b) and 3(c)] that the peaks of the curves do not necessarily correspond to a particular pixel value which is reasonable and expected. The wavelength of the 640.0 nm line was also independently verified using an HP 70951B optical spectrum analyzer.

In summary, the different configurations and the corresponding resolutions of the miniature spectrometer for a pair of wavelengths are as follows:

Table 1. Different set-ups and the corresponding resolution calculated using a pair of wavelengths

No	*f*	Dimensions of the optical part of the spectrometer (includes CCD array but excludes CCD electronics)	Resolution, $\Delta\lambda$	Wavelengths for finding resolution
1	14 cm	16 cm × 4 cm × 4 cm	0.2 nm	514.5 nm , 632.8 nm
2	2 cm	2.5 cm × 0.8 cm × 0.8 cm (1.6 cubic cm)	0.2 nm	632.8 nm, 640 nm
3	1 cm	1.2 cm × 0.4 cm × 0.4 cm (0.19 cubic cm)	0.3 nm	632.8 nm, 640 nm
4[14]	1 cm	same as above	0.51 nm	514.5 nm , 632.8 nm
5	1 cm	same as above	0.66 nm	488 nm, 632.8 nm

The diffraction-limited spot size, D can be calculated from the effective f-number $f\#_{eff}$ as $D = 2.44 \times \lambda \times f\#_{eff}$ where $f\#_{eff} = f/W$ and W is the width of the grating (2.5 mm). D at 632.8 nm for the 14 cm, 2 cm and 1 cm lenses are ~ 86.5, 12.35 and 6.2 μm respectively. It can be observed from entries 3, 4 and 5 of table 1 that the resolution does not depend only on the diffraction-limited spot size. Other factors that affect the resolution are the lens aberrations and the aberrations that arise due to the planar nature of the CCD surface (which we shall call geometrical aberrations). It is to be noted that even though the CCD, which is nothing but a line in one dimension, is adjusted for the position that catches the mid-points of both the sharply focused arcs, the FWH maxima at these points are not exactly equal to the diffraction-limited FWH maxima because the mid-points are not really 'points' but very small 'arc segments' and it is the projections of these arc segments on the CCD that determine the FWH maxima (geometrical aberrations). The geometrical aberrations are dependent on the lens aberrations apart from the location of the CCD and they increase with lens aberrations. The aberrations on the whole increase as the separation between the pair of wavelengths increases. This can be observed from entries 3, 4 and 5 in table 1 where, with the same lens ($f = 1$ cm), the resolution for a pair of wavelengths gets worse as the difference between the wavelengths increases. Nonetheless, it can be stated that with the 1 cm lens, the resolution is below 1 nm for any pair of wavelengths and thereby for any single wavelength between 488.0 nm and 632.8 nm since it is below 1 nm for the edge wavelengths (this pair suffers the maximum aberrations). Also, it can be observed from entries 2 and 3 and entries 1 and 4 of table 1 that the resolution for the same pair of wavelengths worsens as the focal length of the lens (and thereby size) gets smaller and this can be attributed to increased geometrical aberrations. The diffraction-limited spot size, on the other hand, decreases as the focal length gets smaller but since the separation between wavelengths also gets proportionately smaller, the diffraction-defined resolution or FWHM ($\Delta\lambda$) remains the same.

In the final experiment, He-Ne laser light at 632.8 nm and multiple Ar laser lines at 496.5 nm, 501.7 nm and 514.5 nm were combined at the beam splitter and given to the input of the miniature spectrometer. After fixing the CCD position to focus two of the wavelengths sharply (501.7 nm, 632.8 nm), the resulting spectra [Fig. 4(a)] were analyzed as follows. First the background noise was subtracted and then, a parabolic fit was done on the obtained FWHM values for all the different wavelengths. The largest FWHM or in other words, the

#68838 - $15.00 USD Received 13 March 2006; revised 20 April 2006; accepted 25 April 2006

worst possible resolution in that configuration was found to be 19 pixels or 4.6 nm at λ = 568.9 nm [Fig. 4(b)].

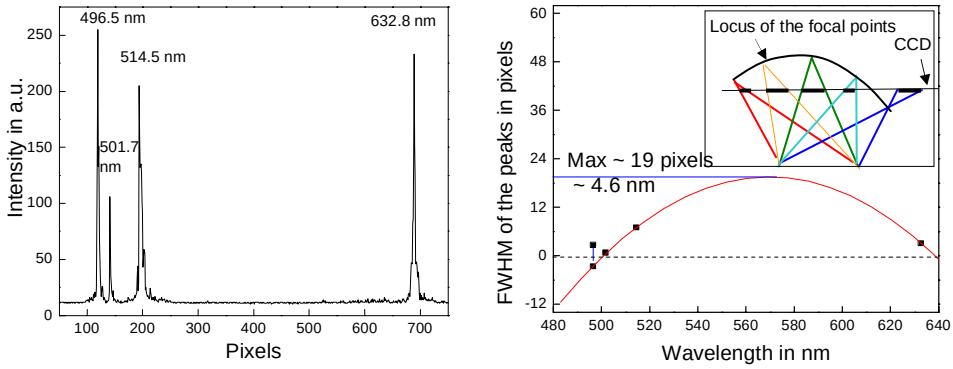

Fig. 4. (a) Multiple wavelengths without background reduction (b) Parabolic approximation to find the resolution, Δλ of the miniature spectrometer Inset shows the intersection of the rays corresponding to different wavelengths with the CCD plane (The picture is exaggerated for the purpose of clarity).

The midpoints of the focused arcs of different wavelengths are localized along an arc whereas the CCD array is a planar surface intersecting this arc [see inset of Fig. 4(b)]. For the case of multiple wavelengths within a range with CCD position fixed as above, the FWH maxima defined by geometrical aberrations are much higher than those defined by the diffraction limit irrespective of the CCD position. A parabolic fit is appropriate for finding the worst resolution because the lengths of the line segments [darkened for highlighting purpose in the inset of Fig. 4(b)] formed by the projections on the CCD of the mid-points of the arcs corresponding to different wavelengths follow a parabola. It is to be noted here that for those points (FWH maxima) lying outside the two minima of the parabola, their images with respect to the horizontal at zero are used for the parabolic fit since it is these images but not the original points that form the parabola. For this reason, in Fig. 4(b), the image of the FWHM for 496.5 nm was taken for the parabolic fit but not the actual obtained FWHM. But, it is to also be noted that the actual resolution or FWHM for all the wavelengths is always positive. This is a very reasonable estimation for the worst possible resolution since the parabolic fit passes through all the four experimentally obtained points. This worst case resolution (4.6 nm) in a fixed CCD position is similar to that (5 nm) achieved in [9] but in a 1.5 times wider spectral range (150 nm). By adjusting the CCD position for maximum resolution for each pair of peaks as described earlier, a sub-nm resolution is achieved in the case of multiple wavelengths also.

An estimation of the throughput of the device was done as follows: He-Ne laser light (λ = 632.8 nm) of diameter 2 mm was focused normally on the waveguide grating with the help of a 12 cm focal length lens resulting in a spot of diameter ~ 93μm on the grating. By slowly rotating the sample, the angle of incidence was adjusted to the value where maximum coupling into the waveguide was observed. At this position, the He-Ne laser light track inside the waveguide could be seen. By placing a photodetector very close to the waveguide edge, the output power coming from the edge was measured. This was 12 μW whereas the incident beam power was 1.272 mW. Hence, the throughput was estimated as 0.94 %. Nonetheless, spectra from weak, non-coherent sources can be successfully observed by integrating several successive frames of the CCD (frame rate 30 fps). Further improvement can be done by reducing the waveguide losses (measured loss for our waveguide is 2.2 dB/cm) and

#68838 - $15.00 USD Received 13 March 2006; revised 20 April 2006; accepted 25 April 2006

optimizing the grating depth for maximum throughput also in combination with maximum resolution.

Drawing an analogy to a conventional grating-based Czerny-Turner type monochromator spectrometer, the maximum input slit width for our spectrometer in the direction of the normal to the grating [y-axis in fig. 5(a)] is limited by the effective width of the waveguide and that along the direction of the grating groove orientation [x-axis in fig. 5(a)] is limited by the grating length (~ 4 mm). Unlike in a conventional spectrometer, the width of the input slit (in both x and y directions) does not affect the resolution of our spectrometer since increasing or decreasing the slit width does not change the effective number of grooves contributing to dispersion. This gives an advantage over conventional spectrometers when detecting weak signals since the slit width can be increased to collect more light by simply increasing the grating length thus improving the throughput without affecting the resolution of the device at all. The resolution does not also depend on the aperture of the light coming through the input slit for the same reason. A greater aperture simply results in a longer arc at the CCD in our case. It is to be noted that the light inside the waveguide in our resolution experiments is not collimated (it is diverging starting from the front facet of the waveguide) and therefore resulted in the arcs. Perfectly collimated light in the waveguide is expected to be focused as a point on the CCD plane [blue light in fig. 5(a)]. Light from an uncollimated beam [red beam in fig. 5(a)] would be clearly resolved by our integrated-optic spectrometer since every light ray in the beam is totally internally reflected and thereby presents a collimated set of rays to the grooves encountered in its direction. Also, regardless of the point of origin of the divergent light ray on the slit and the angle α that it makes with respect to the z-axis, it will be focused as a point along the fixed arc defined by the wavelength λ of the light and the grating periodicity Λ as shown in fig. 5(b). This is another clear advantage over a conventional spectrometer in which a collimator is a must. By further developing an algorithm for integrating the CCD pixel intensities along these arcs, the throughput of the device can be effectively improved by a factor equal to the number of pixel rows on the CCD (480 in this particular case).

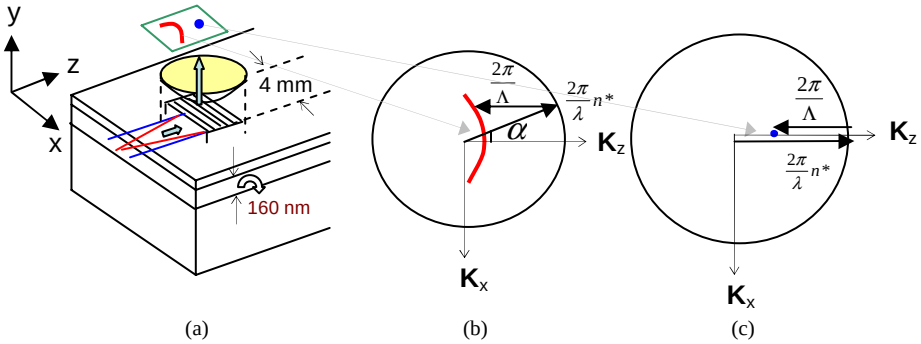

Fig. 5. (a) Collimated (blue) and uncollimated light (red) and the outcoupled spectra on the CCD (b) Wave vectors in the x-z plane and the resulting spectrum for an uncollimated beam (c) Wave vectors in the x-z plane and the resulting spectrum for a collimated beam

It is recalled here that only the TE_0 guided mode in the waveguide was studied in all the above experiments. Polarization of the incident light is not a concern in conventional grating-based Czerny-Turner type spectrometers but it becomes important in an integrated optic grating based spectrometer like ours. This is because the TE and the TM polarizations of the guided mode give rise to slightly different effective indices of the waveguide and hence, result in slightly different out-coupling angles for the different wavelengths (about 5^o in our case). This leads to undesirable overlap of the output spectra affecting the resolution when the input

#68838 - $15.00 USD Received 13 March 2006; revised 20 April 2006; accepted 25 April 2006

light has both TE and TM polarization components which is a common case for spectroscopy samples. Hence, to complete this design, it has to be made polarization independent or very low–polarization dependent for the entire wavelength range of its operation. An effective solution for our design is one that still retains the integrated optic nature and thereby the compactness of our device. Previous work [16, 17] suggests a high insertion loss (> 40 dB) for TM polarization with a very low insertion loss for TE polarization obtained with a metal coating with or without a buffer layer on a planar waveguide. We plan to explore this completely integrated-optic solution for our miniature spectrometer.

6. Conclusion

The combination of integrated-optics (planar geometry) and micro-optics (free space geometry) resulted in a compact miniature spectrometer design. With optical part occupying only 0.2 cubic cm, the miniature spectrometer gives sub-nm resolution in the 488.0 nm – 632.8 nm wavelength region. The flexibility and ease in adjusting the CCD position make the aforementioned sub-nm resolution possible. The worst possible resolution with the CCD position fixed to always sharply capture two wavelengths in the above range has been found to be 4.6 nm. Our miniature spectrometer provides an order of resolution better than other grating-based spectrometers of similar size and in a wider wavelength span. There is scope for further improvement of our design by replacing the CCD with much smaller and better CMOS camera.

Since this miniature spectrometer gives real-time images to a computer which analyzes them for resolution and other information, online or in-situ measurements can also be done easily. The planar waveguide design makes it very well suited for the integration of micro-fluidic channels and lab-on-a-chip applications. Nano imprinting, nano embossing and other advances in grating manufacturing technologies have made bulk manufacturing of sub-micron gratings easier. Our design which is based on uniform period grating and off-the-shelf plano-convex lens is not only cost-effective and easy to fabricate and assemble but also feasible for bulk-manufacturing. By simply varying the periodicity of the uniform period grating, the wavelength range of this miniature spectrometer can be varied to other ranges in the visible wavelength range or even the infrared range. The simplicity, flexibility and ease of fabrication are clear advantages over MEMS, CMOS, MOEMS or other IO designs and those that employ grating lenses. Our miniature spectrometer serves as a quick and easy solution for many spectrometric applications that also works very well.

Acknowledgments

This work was supported by U.S. Army TACOM DAAE07-03-C-L140. The authors would like to thank Mark Murray for his guidance in silica dry etching.

#68838 - $15.00 USD Received 13 March 2006; revised 20 April 2006; accepted 25 April 2006